

# Three-Coordinate, 12-Electron Organometallic Complexes of Iron(II) Supported by a Bulky $\beta$ -Diketimate Ligand: Synthesis and Insertion of CO To Give Square-Pyramidal Complexes

Jeremy M. Smith, Rene J. Lachicotte, and Patrick L. Holland\*

Department of Chemistry, University of Rochester, Rochester, New York 14627

Received July 16, 2002

The preparation of a series of three-coordinate, 12-electron organometallic complexes of iron(II) supported by a bulky  $\beta$ -diketimate ligand is described. The thermally stable complexes  $\text{LFeR}$  ( $\text{R} = \text{Et}$ ,  $\text{CH}_2^t\text{Bu}$ ,  $^i\text{Pr}$ ) are three-coordinate in both the solid state (single crystal X-ray diffraction) and solution. They react rapidly with CO to form the diamagnetic complexes  $\text{LFe}(\text{CO})_2(\text{COR})$ , which have an unusual square-pyramidal geometry. Spectroscopic and crystallographic studies show that the acyl group is in the axial position. As a result, there are two orientations of the acyl group about the  $\text{Fe}-\text{C}$  bond, and the isomeric ratio is dependent on the size of R. The two isomers are in equilibrium in solution at room temperature.

## Introduction

Low-coordinate, coordinatively unsaturated late-transition-metal complexes are often invoked as reactive intermediates in catalytic processes. In the case of iron, low-coordinate metal centers have been proposed as the active species in alkene polymerization<sup>1,2</sup> as well as C–H activation<sup>3–5</sup> and functionalization<sup>6,7</sup> processes.

Stable three-coordinate complexes are rare in compounds with less than 10 d electrons.<sup>8,9</sup> Most three-coordinate complexes of iron are homoleptic, and reactions of these complexes tend to be at the expense of the low coordination number.<sup>8</sup> Few reported three-coordinate ferrous complexes contain  $\text{Fe}-\text{C}$  bonds. Among these are the dimeric diaryl complexes  $[\text{FeR}_2]_2$  ( $\text{R} = 2,4,6\text{-Me}_3\text{C}_6\text{H}_2$ ,  $2,4,6\text{-}^i\text{Pr}_3\text{C}_6\text{H}_2$ ) and their monomeric adducts  $\text{FeR}_2\text{L}$  ( $\text{L} = \text{donor ligand}$ )<sup>10–14</sup> and the N-functionalized alkyl complex  $\text{Fe}_2(\eta^2\text{-CHSi}^t\text{BuMe}_2\text{C}_5\text{H}_4\text{N-2})_4$ .<sup>15</sup>

We have recently shown that the bulky  $\beta$ -diketimate ligand 2,2,6,6-tetramethyl-3,5-bis((2,6-diisopropylphenyl)imido)hept-4-yl leads to isolable three-coordinate complexes of iron, cobalt, and nickel (Figure 1).<sup>16,17</sup> Since only two donor atoms exert the steric hindrance in these complexes, it is possible to prepare heteroleptic three-coordinate complexes in which the third coordination site is occupied by a chloride ligand. Selective reaction of the chloride ligand gives products in which the low coordination number at the metal is maintained. Thus, for example, it is possible to prepare three-coordinate complexes of iron and cobalt in which methyl ligands occupy the third coordination site.<sup>17,18</sup> Other researchers have also used  $\beta$ -diketimate ligands to prepare paramagnetic organometallic complexes,<sup>19–22</sup> albeit with greater coordination numbers.

This contribution shows that the synthetic method used for  $\text{LFeMe}$  is generally applicable for creating a series of stable three-coordinate, 12-electron organometallic complexes of iron. We also report initial reactivity studies of our three-coordinate alkyl complexes with the prototypical organometallic ligand CO. In contrast to the more common 18-electron organometallic complexes, low-electron-count, coordinatively unsaturated organometallic complexes have not been as extensively stud-

\* To whom correspondence should be addressed. E-mail: holland@chem.rochester.edu.

(1) Britovsek, G. J. P.; Gibson, V. C.; Wass, D. F. *Angew. Chem., Int. Ed.* **1999**, *38*, 428–447.

(2) Ittel, S. D.; Johnson, L. K.; Brookhart, M. *Chem. Rev.* **2000**, *100*, 1169–1203.

(3) Baker, M. V.; Field, L. D. *J. Am. Chem. Soc.* **1987**, *109*, 2825–2826.

(4) Field, L. D.; George, A. V.; Messerle, B. A. *J. Chem. Soc., Chem. Commun.* **1991**, 1339–1341.

(5) Whittlesey, M. K.; Mawby, R. J.; Osman, R.; Perutz, R. N.; Field, L. D.; Wilkinson, M. P.; George, M. W. *J. Am. Chem. Soc.* **1993**, *115*, 8627–8637.

(6) Waltz, K. M.; Muhoro, C. N.; Hartwig, J. F. *Organometallics* **1999**, *18*, 3383–3393.

(7) Waltz, K. M.; Hartwig, J. F. *J. Am. Chem. Soc.* **2000**, *122*, 11358–11369.

(8) Cummins, C. C. *Prog. Inorg. Chem.* **1998**, *47*, 685–836.

(9) Alvarez, S. *Coord. Chem. Rev.* **1999**, *193–195*, 13–41.

(10) Machelett, B. Z. *Chem.* **1976**, *16*, 116.

(11) Seidel, W.; Lattermann, K.-J. *Z. Anorg. Allg. Chem.* **1982**, *488*, 69–74.

(12) Müller, H.; Seidel, W.; Görls, H. *J. Organomet. Chem.* **1993**, *445*, 133–136.

(13) Klose, A.; Solari, E.; Ferguson, R.; Floriani, C.; Chiesi-Villa, A.; Rizzoli, C. *Organometallics* **1993**, *12*, 2414–2416.

(14) Klose, A.; Solari, E.; Floriani, C.; Chiesi-Villa, A.; Rizzoli, C.; Re, N. *J. Am. Chem. Soc.* **1994**, *116*, 9123–9135.

(15) Leung, W.-P.; Lee, H. K.; Weng, L.-H.; Luo, B.-S.; Zhou, Z.-Y.; Mak, T. C. W. *Organometallics* **1996**, *15*, 1785–1792.

(16) Smith, J. M.; Lachicotte, R. J.; Holland, P. L. *Chem. Commun.* **2001**, 1542–1543.

(17) Holland, P. L.; Cundari, T. R.; Perez, L. L.; Eckert, N. A.; Lachicotte, R. J. *J. Am. Chem. Soc.*, in press.

(18) Andres, H.; Bominaar, E. L.; Smith, J. M.; Eckert, N. A.; Holland, P. L.; Münck, E. *J. Am. Chem. Soc.* **2002**, *124*, 3012–3025.

(19) Kim, W.-K.; Fevola, M. J.; Liable-Sands, L. M.; Rheingold, A. L.; Theopold, K. H. *Organometallics* **1998**, *17*, 4541–4543.

(20) Theopold, K. H.; Kim, W.-K.; Power, J. M.; Mora, J. M.; Masino, A. P. Patent WO 2001012637 (2000).

(21) Gibson, V. C.; Newton, C.; Redshaw, C.; Solan, G. A.; White, A. J. P.; Williams, D. J. *Eur. J. Inorg. Chem.* **2001**, 1895–1903.

(22) MacAdams, L. A.; Kim, W.-K.; Liable-Sands, L. M.; Guzei, I. A.; Rheingold, A. L.; Theopold, K. H. *Organometallics* **2002**, *21*, 952–960.

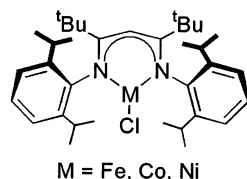
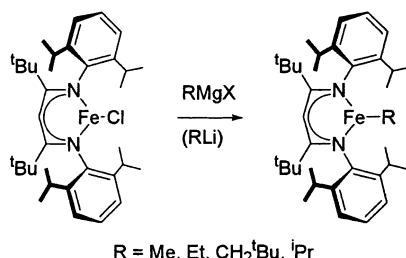


**Figure 1.** Three-coordinate chloride complexes supported by a bulky  $\beta$ -diketiminato ligand.

**Scheme 1**



ied.<sup>23,24</sup> The three-coordinate  $[\text{FeR}_2]_2$  complexes mentioned above undergo insertion reactions with isocyanides and nitriles.<sup>13,14</sup> There are a few examples of 14-electron, 4-coordinate organometallic complexes of iron.<sup>15,25–32</sup> Among the most extensively studied are the 1,2-bis-(diisopropylphosphino)ethane complexes  $\text{Fe}(\text{dippe})\text{R}_2$  and  $\text{Fe}(\text{dippe})(\text{R})\text{Cl}$ , which display reactivity patterns similar to those of 18-electron complexes,<sup>27,28,33</sup> and the hydrotris(3,5-diisopropylpyrazolyl)borate complexes  $\text{Fe}(\text{Tp}^{i\text{Pr}})\text{R}$ , which display some unusual properties, such as stability toward  $\beta$ -hydride elimination.<sup>31,32</sup>

## Results and Discussion

**Synthesis and Characterization of 3-Coordinate Iron(II) Alkyl Complexes.** Preparation of the three-coordinate organometallic complexes  $\text{LFeR}$  ( $\text{R} = \text{Me}, \text{Et}, \text{CH}_2^t\text{Bu}, i\text{Pr}$ ) was achieved by reaction of the three-coordinate chloride complex  $\text{LFeCl}$ <sup>16</sup> with the appropriate Grignard or alkyllithium reagent in ether solutions at room temperature (Scheme 1). The preparation and characterization of  $\text{LFeMe}$  has been previously reported.<sup>18</sup> The organometallic complexes were isolated as orange solids in high yield by crystallization from pentane solutions at  $-35^\circ\text{C}$ . Bulky alkyl groups are not required, as is evident from the isolation of  $\text{LFeMe}$ .

The low-coordinate nature of the iron atom in all complexes was confirmed by X-ray crystallographic

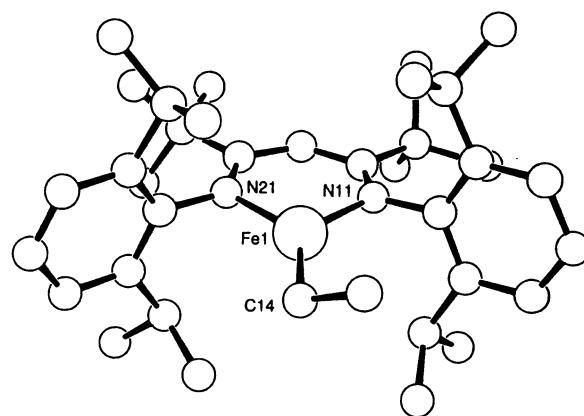


**Figure 2.** Ball and stick diagram of the complex  $\text{LFeEt}$ . Hydrogen atoms are omitted for clarity.

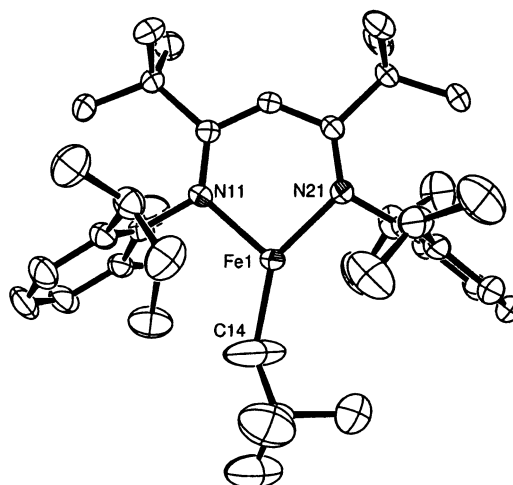


**Figure 3.** ORTEP diagram of the complex  $\text{LFeCH}_2^t\text{Bu}$ . Hydrogen atoms are omitted for clarity; thermal ellipsoids are given at the 50% probability level.

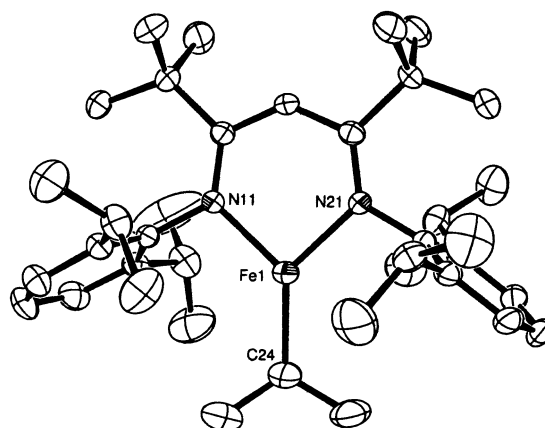


**Figure 4.** ORTEP diagram of the complex  $\text{LFe}^i\text{Pr}$ . Hydrogen atoms are omitted for clarity; thermal ellipsoids are given at the 50% probability level.

studies (Figures 2–4). In the case of  $\text{LFeEt}$ , suspected twinning problems led to high residuals ( $R1 = 0.15$ ), but we were able to confirm the connectivity of the molecule. The experimental data and selected structural parameters are listed in Tables 1 and 2. All complexes are three-coordinate in the solid state. For the complexes  $\text{LFeCH}_2^t\text{Bu}$  and  $\text{LFe}^i\text{Pr}$ , confirmation of the trigonal-planar geometry is obtained from the sum of

(23) Theopold, K. H. *Acc. Chem. Res.* **1990**, *23*, 263–270.

(24) Poli, R. *Chem. Rev.* **1996**, *96*, 2135–2204.

(25) Akita, M.; Shirasawa, N.; Hikichi, S.; Moro-oka, Y. *Chem. Commun.* **1998**, 973–974.

(26) Fryzuk, M. D.; Leznoff, D. B.; Ma, E. S. F.; Rettig, S. J.; Young, V. G., Jr. *Organometallics* **1998**, *17*, 2313–2323.

(27) Hermes, A. R.; Girolami, G. S. *Organometallics* **1987**, *6*, 763–768.

(28) Hermes, A. R.; Girolami, G. S. *Organometallics* **1988**, *7*, 394–401.

(29) Kisko, J. L.; Hascall, T.; Parkin, G. *J. Am. Chem. Soc.* **1998**, *120*, 10561–10562.

(30) Hursthouse, M. B.; Izod, K. J.; Motevalli, M.; Thornton, P. *Polyhedron* **1996**, *15*, 135–145.

(31) Shirasawa, N.; Akita, M.; Hikichi, S.; Moro-oka, Y. *Chem. Commun.* **1999**, 417–418.

(32) Shirasawa, N.; Nguyen, T. T.; Hikichi, S.; Moro-oka, Y.; Akita, M. *Organometallics* **2001**, *20*, 3582–3598.

(33) Hermes, A. R.; Warren, T. H.; Girolami, G. S. *J. Chem. Soc., Dalton Trans.* **1995**, 301–305.

**Table 1. Experimental Data for X-ray Diffraction Studies of LFeR (R = CH<sub>2</sub><sup>t</sup>Bu, <sup>i</sup>Pr) and LFe(CO)<sub>2</sub>(COMe)**

	LFeCH <sub>2</sub> <sup>t</sup> Bu	LFe <sup>i</sup> Pr	LFe(CO) <sub>2</sub> (COMe)
formula	C <sub>40</sub> H <sub>64</sub> FeN <sub>2</sub>	C <sub>38</sub> H <sub>60</sub> FeN <sub>2</sub>	C <sub>39</sub> H <sub>55</sub> FeN <sub>2</sub> O <sub>3</sub>
fw	628.78	600.73	655.70
cryst size (mm)	0.18 × 0.32 × 0.44	0.20 × 0.26 × 0.38	0.02 × 0.20 × 0.24
<i>a</i> (Å)	9.7226(7)	9.6306(6)	9.5385(8)
<i>b</i> (Å)	18.187(1)	17.388(1)	12.519(1)
<i>c</i> (Å)	21.785(2)	21.749(1)	17.043(2)
α (deg)	90	90	72.705(2)
β (deg)	96.771(1)	95.884(1)	82.442(2)
γ (deg)	90	90	67.729(1)
<i>V</i> (Å <sup>3</sup> )	3825.5(5)	3623.0(4)	1797.8(3)
<i>Z</i>	4	4	2
space group	<i>P</i> 2 <sub>1</sub> / <i>n</i>	<i>P</i> 2 <sub>1</sub> / <i>n</i>	<i>P</i> $\bar{1}$
<i>T</i> (K)		193	
λ (Å)		0.710 73 (Mo Kα)	
μ (mm <sup>-1</sup> )	0.421	0.442	0.457
ρ <sub>calcd</sub> (g cm <sup>-3</sup> )	1.092	1.101	1.211
R1 <sup>a</sup>	0.063	0.068	0.068
wR2 <sup>a</sup>	0.182	0.155	0.146
GOF <sup>b</sup>	1.011	1.073	1.109

<sup>a</sup> R1 =  $(\sum [|F_o| - |F_c|] / |F_o|)$ ; wR2 =  $(\sum [w(F_o^2 - F_c^2)^2] / \sum [w(F_o^2)^2])^{1/2}$ , where  $w = 1/[\sigma^2(F_o^2) + (aP)^2 + bP]$  and  $P = [\text{Max}\{0, F_o^2\} + 2F_c^2] / 3$ . <sup>b</sup> GOF =  $(\sum [w(F_o^2 - F_c^2)^2 / (n - p)])^{1/2}$ , where *n* and *p* denote the numbers of data and parameters, respectively.

**Table 2. Selected Bond Lengths (Å) and Angles (deg) for the Complexes LFeR**

	LFeMe	LFeCH <sub>2</sub> <sup>t</sup> Bu	LFe <sup>i</sup> Pr
Fe–C	2.009(3)	2.027(4)	2.048(3)
Fe–N	1.973(1)	1.996(2)	1.994(2)
		1.994(2)	1.995(2)
N–Fe–C	132.57(4)	120.4(2)	130.8(1)
		142.9(2)	134.5(1)
N–Fe–N (bite angle)	96.4(1)	94.62(7)	94.10(8)
C–N–C	128.56(1)	126.3(2)	125.5(2)
		127.9(2)	127.6(2)
N...N	2.906(3)	2.933(3)	2.920(3)
fold angle <sup>a</sup>	0.49 (0.06)	0.71 (0.36)	1.50 (0.38)

<sup>a</sup> Angle between the least-squares NCCCN and NMN planes of the six-membered diketiminate–metal ring.

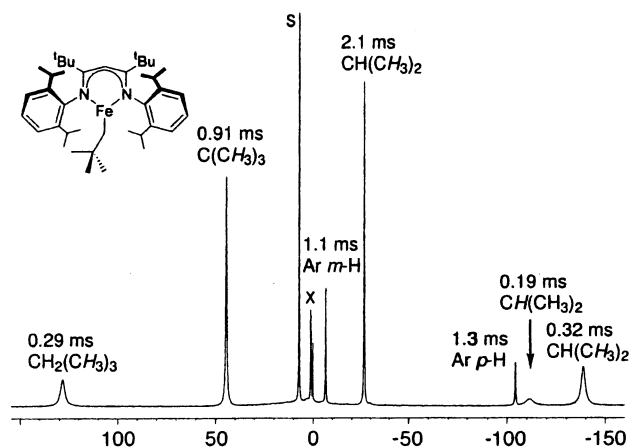
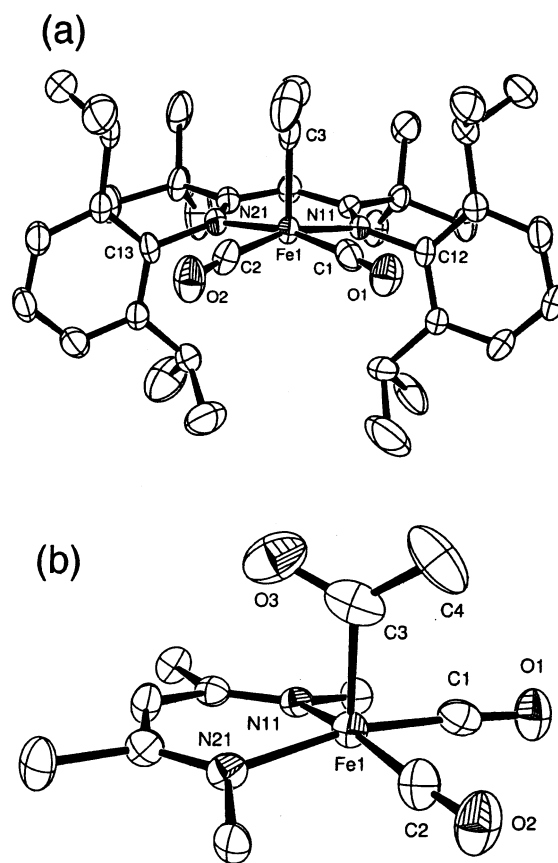
bond angles around iron (~360°). There are no agostic interactions in either molecule, as the closest intramolecular Fe...H–C contact is 2.70 Å. From the data in Table 1, it is evident that the larger alkyl groups are accommodated solely by an increase in the iron–carbon distance. The bulkier alkyl groups do not cause a decrease in the bite angle, force the aryl groups to bend away from the alkyl ligand (C–N–C angle), or change the geometry of the rigid diketiminate ligand (N...N distance).

A number of three-coordinate iron β-diketiminate complexes have been crystallographically characterized. The Fe–N bond lengths in all these complexes are similar to each other (~2.0 Å)<sup>16–18,34,35</sup> and similar to those of the alkyl complexes reported here. The low coordination number of the metal center results in remarkably short Fe–C bond lengths (2.009(3)–2.048(3) Å).<sup>17,36</sup> A three-coordinate iron benzyl complex supported by a less bulky β-diketiminate ligand<sup>16</sup> has an Fe–C bond length of 2.042(2) Å.<sup>35</sup>

(34) Panda, A.; Stender, M.; Wright, R. J.; Olmstead, M.; Klavins, P.; Power, P. P. *Inorg. Chem.* **2002**, *41*, 3909–3916.

(35) Sciarone, T. J. J.; Meetsma, A.; Hessen, B.; Teuben, J. H. *Chem. Commun.* **2002**, 1580–1581.

(36) Balch, A. J.; Olmstead, M.; Safari, N.; St. Clair, T. N. *Inorg. Chem.* **1994**, *33*, 2815–2822.

**Figure 5.** <sup>1</sup>H NMR spectrum of the complex LFeCH<sub>2</sub><sup>t</sup>Bu. Approximate *T*<sub>2</sub> values and assignments are indicated (s, residual C<sub>6</sub>D<sub>5</sub>H; x, solvent impurities).**Figure 6.** (a) ORTEP diagram of the complex LFe(CO)<sub>2</sub>-(COMe). Hydrogen atoms are omitted for clarity; thermal ellipsoids are given at the 50% probability level. (b) Expanded view of the β-diketiminate ring, showing the square-pyramidal geometry around the metal. Aromatic rings on the nitrogen atoms and *tert*-butyl groups on the ligand backbone are omitted for clarity.

All complexes are paramagnetic, with solution magnetic moments around 5.5 μ<sub>B</sub>, suggestive of high-spin iron(II) (*S* = 2).<sup>18</sup> Consistent with the high-spin nature of the compounds, the <sup>1</sup>H NMR spectra show paramagnetically shifted resonances. The solution <sup>1</sup>H NMR spectrum of the complex LFeCH<sub>2</sub><sup>t</sup>Bu in benzene-*d*<sub>6</sub> (Figure 5) is representative. The spectrum is consistent with the solid-state structure: signals from all protons in the complex are observed, with the exception of those



on the  $\alpha$ -carbon of the alkyl group, most likely due to their close proximity to the paramagnetic iron center. Most of the resonances can be assigned on the basis of their relative integration,<sup>17</sup> although by this criterion alone we cannot distinguish the two sets of chemically inequivalent isopropyl methyl protons. However, we have previously shown that the distance of the protons from the paramagnetic center can be correlated with both the chemical shift and relaxation time of the peak (estimated from peak broadness).<sup>17,37</sup> Thus, the resonance at  $\delta -140$  can be assigned to the two methyl groups adjacent to the iron atom, and the peak at  $\delta -30$  can be assigned to the methyl groups closer to the backbone of the ligand. Similarly, we assign the peak at  $\delta -111$  to the four methine protons and the peak at  $\delta -4.5$  to the four aryl protons meta to the nitrogen atoms. Similarly for the other alkyl complexes, signals for all the protons of the  $\beta$ -diketiminate ligand were observed, while the protons of the alkyl ligand in close proximity ( $\alpha$  or  $\beta$  to iron) to the metal center were not observed.

The UV-vis spectra in pentane solution all show a peak at around 520 nm, with a molar extinction coefficient of  $0.51\text{--}0.58\text{ mM}^{-1}\text{ cm}^{-1}$ . This peak is characteristic of the alkyl complexes and has not been observed in the UV-vis spectra of other three-coordinate  $\beta$ -diketiminate iron complexes.<sup>16,17,38</sup>

Although highly sensitive to oxygen and water, the complexes are all thermally stable. The  $^1\text{H}$  NMR spectrum of the methyl complex  $\text{LFeMe}$  showed no changes after heating for 3 days at  $120^\circ\text{C}$ . The complex also survives hydrogenation pressures of up to 2000 psi unscathed. Even more remarkably, the complex  $\text{LFeEt}$  showed no propensity toward  $\beta$ -hydride elimination. No changes in the  $^1\text{H}$  NMR spectrum were observed either on heating at  $120^\circ\text{C}$  for 3 days or after irradiation with visible light.

One possible explanation for the compounds' resistance to thermal degradation is the highly crowded nature of the metal center. However, we have been able to prepare complexes with coordination number 5 having ligands residing between the two aryl rings of the  $\beta$ -diketiminate ligand (see below), suggesting that the diketiminate iron moiety can accommodate further ligands. A second possible explanation is that in these high-spin complexes<sup>18</sup> there are no empty orbitals on the metal and, therefore,  $\beta$ -hydride elimination reactions are not possible.<sup>24</sup> This explanation has been used to rationalize the observation that tetrahedral 14-electron iron alkyl complexes supported by hydrotris-(3,5-diisopropylpyrazolyl)borato and hydrotris(3,4,5-trimethylpyrazolyl)borato ligands are resistant to  $\beta$ -hydride elimination.<sup>29,31,32</sup>

### Carbonylation of 3-Coordinate Alkyl Complexes.

Exposure of an orange solution of  $\text{LFeMe}$  to an atmosphere of CO led to the formation of a red diamagnetic product (Scheme 2), which was characterized as the 5-coordinate complex  $\text{LFe}(\text{CO})_2(\text{COMe})$  and was observed in a 2:1 isomeric mixture. The acyl-dicarbonyl functionality shows a characteristic set of absorbances

Scheme 2

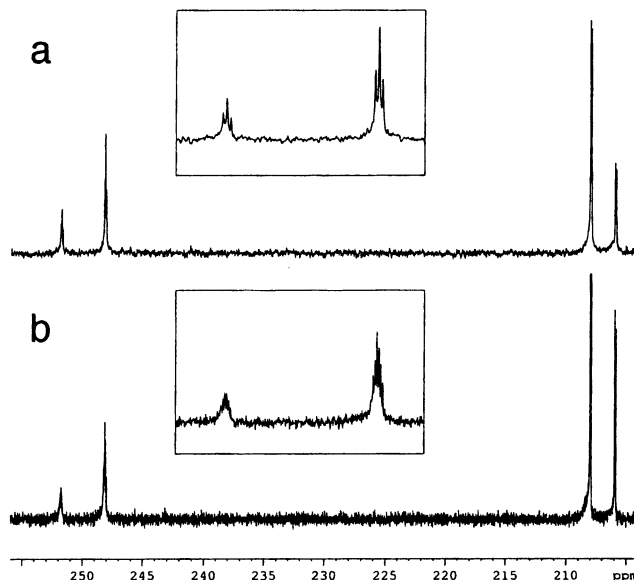
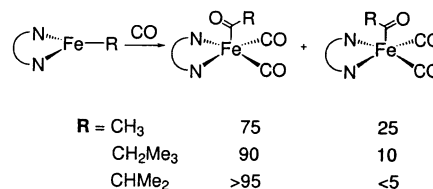


**Figure 7.** (a)  $^{13}\text{C}\{^1\text{H}\}$  NMR spectrum of the complex  $\text{LFe}-(^{13}\text{CO})_2(^{13}\text{COMe})$ . The inset shows an expansion of the signals for the acyl methyl groups. (b)  $^{13}\text{C}$  NMR spectrum of the complex  $\text{LFe}-(^{13}\text{CO})_2(^{13}\text{COMe})$ . The inset shows an expansion of the signals for the acyl methyl groups.

in the IR spectrum. The major product showed a single  $\nu_{\text{C=O}}$  absorption ( $1687\text{ cm}^{-1}$ ) and two  $\nu_{\text{CO}}$  absorptions ( $1998, 1934\text{ cm}^{-1}$ ). In the  $^1\text{H}$  NMR spectrum of this product the methine protons of the isopropyl groups give two sets of signals at  $\delta 3.52$  and  $2.58$ , suggesting loss of symmetry about the iron-diketiminate ligand plane. In the  $^{13}\text{C}\{^1\text{H}\}$  NMR spectrum of the complex prepared from  $^{13}\text{CO}$  (Figure 7), the acyl ligand carbon resonates as a triplet at  $\delta 248.1$ , which is further split by coupling to the methyl protons in the proton-coupled  $^{13}\text{C}$  spectrum. The two terminal carbonyl ligands resonate together as a doublet at  $\delta 208.0$ , suggesting the presence of a mirror plane in the molecule. The spectroscopic data are consistent with a square-pyramidal geometry in which the carbonyl ligands occupy the basal positions. This is confirmed by estimating the angle between the two carbonyl groups in the isomers using the relation  $\tan^2 \theta = I_{\text{as}}/I_{\text{s}}$ , where  $2\theta$  is the angle between the two carbonyl bands,  $I_{\text{s}}$  is the height of the symmetric  $\nu_{\text{CO}}$  band, and  $I_{\text{as}}$  is the height of the asymmetric  $\nu_{\text{CO}}$  band.<sup>39</sup> For the major isomer,  $\theta = 86^\circ$ , and for the minor isomer,  $\theta = 90^\circ$ . The minor product shows similar features in its IR and NMR spectra and, thus is also proposed to have a square-pyramidal structure with the acyl group in the apical position.

The 2D NOESY/EXSY spectrum evidences chemical exchange between the isomers. For example, a positive

(37) Ming, L.-J. In *Physical Methods in Bioinorganic Chemistry*; Que, L., Jr., Ed.; University Science Books: Sausalito, CA, 2000; pp 375–464.

(38) Smith, J. M.; Eckert, N. A.; Holland, P. L. Unpublished results.

(39) Beck, W.; Melnikoff, A.; Stahl, R. *Angew. Chem., Int. Ed. Engl.* **1965**, *4*, 692–693.

**Table 3. Selected Bond Lengths (Å) and Angles (deg) for the Complex  $\text{LFe}(\text{CO})_2(\text{COMe})$** 

Fe(1)–C(1)	1.774(6)	Fe(1)–N(11)	1.983(4)
Fe(1)–C(2)	1.773(6)	Fe(1)–N(21)	1.989(4)
Fe(1)–C(3)	1.946(6)		
C(1)–Fe(1)–C(2)	81.5(2)	N(11)–Fe(1)–N(21) <sup>a</sup>	94.8(2)
C(1)–Fe(1)–C(3)	92.1(2)	C(21)–N(11)–C(12)	121.9(4)
C(2)–Fe(1)–C(3)	94.4(3)	C(41)–N(21)–C(13)	121.9(4)

<sup>a</sup> Bite angle.

cross-peak is observed between the diketiminate backbone protons of each isomer at  $\delta$  6.67 (major) and  $\delta$  6.39 (minor). Similar positive cross-peaks are observed between the other equivalent protons of each isomer. Since both complexes are square pyramidal, it is likely that they differ by the orientation of the acyl group around the Fe–C bond. Unfortunately, no cross-peaks were observed in the 2D NOESY/EXSY spectrum between the acyl methyl group and the backbone *tert*-butyl groups; therefore, it was not possible to assign the isomers conclusively using 2D NMR.

Both  $\text{LFeCH}_2^t\text{Bu}$  and  $\text{LFe}^i\text{Pr}$  show similar CO insertion chemistry (Scheme 2). Interestingly, the proportion of the major isomer present in the equilibrium mixture increases as the R groups increase in size from neopentyl to isopropyl. This is more consistent with the major isomer having the alkyl group pointed away from the diketiminate ligand backbone, and these assignments are used in Scheme 2.

The solution assignment of  $\text{LFe}(\text{CO})_2(\text{COMe})$  was confirmed by X-ray crystallography (Figure 6). The structure is consistent with the major solution isomer, with the acyl methyl pointed away from the diketiminate backbone. The CO–Fe–CO bond angle  $\theta$ , at  $81.5(2)^\circ$ , compares favorably with the value calculated from the IR spectrum ( $86^\circ$ , see above). In comparison to the alkyl complexes, there is not a significant change in the bond lengths and angles of the diketiminate ligand to the iron center (Table 3), despite the increased coordination number and diamagnetism of the complex. Both the Fe–N bond lengths and the bite angle are similar to those of the starting material. However, the C–N–C bond angles become smaller as the aryl groups are pushed back toward the *tert*-butyl groups on the ligand backbone, allowing more space for other ligands to coordinate. The  $\beta$ -diketiminate ligand further adjusts to accommodate the extra ligands by bending the aryl groups away from the apical acyl ligand. This pulls the methine carbons of the isopropyl groups adjacent to the acyl ligand away from each other to a distance of 6.950(7) Å and pushes the other two methine carbons toward each other so that they are separated by 4.012(7) Å. In the precursor complex  $\text{LFeMe}$  the methine carbons are separated by 5.204(3) Å. It is likely that this deformation sterically prohibits a sixth ligand from coordinating to the iron center.

In a related reaction, Akita has found that the 4-coordinate hydrotris(3,5-diisopropylpyrazolyl)borato- and hydrotris(3,4,5-trimethylpyrazolyl)borato-supported complexes react with CO to give hexacoordinate acyl dicarbonyl complexes,  $\text{TpFe}(\text{CO})_2(\text{COR})$ .<sup>31,32</sup> On the other hand, reaction of a complex supported by the more bulky phenyltris(3-*tert*-butylpyrazolyl)borato ligand results in reduction to the iron(I) complex  $\text{TpFe}(\text{CO})$ .<sup>29</sup>

Carbonylation of the tetrahedral 14-electron complexes  $\text{Fe}(\text{dippe})(\text{R})\text{X}$  similarly led to the formation of the octahedral complexes  $\text{Fe}(\text{dippe})(\text{COR})(\text{CO})_2\text{X}$ . It was possible to isolate the intermediate  $\eta^2$ -acyl complexes  $\text{Fe}(\text{dippe})(\eta^2\text{-COR})(\text{CO})_2\text{X}$  by using a sufficiently bulky R group and controlling the CO stoichiometry.<sup>28</sup> However, we were not able to isolate any intermediates; addition less than 3 equiv of CO to  $\text{LFeR}$  at  $-78^\circ\text{C}$  followed by warming to room temperature resulted only in incomplete formation of the final product.

## Conclusion

Through the use of a suitably bulky  $\beta$ -diketiminate ligand, it is possible to isolate and characterize a series of thermally stable 12-electron iron(II) alkyl complexes. The presence of exposed  $\beta$ -hydrogen atoms does not affect the stability of the complexes. Reactions with CO result in the formation of diamagnetic square-pyramidal complexes, again highlighting the ability of diketiminate ligands to stabilize unusual geometries.<sup>40</sup>

## Experimental Section

**General Procedures.** All manipulations were performed under a nitrogen atmosphere by standard Schlenk techniques or in an M. Braun glovebox maintained at or below 1 ppm of  $\text{O}_2$  and  $\text{H}_2\text{O}$ . Glassware was dried at  $150^\circ\text{C}$  overnight. NMR data were recorded on a Bruker Avance 400 spectrometer (400 MHz) at  $22^\circ\text{C}$ . All peaks in the NMR spectra are reported in ppm, referenced to residual  $\text{C}_6\text{D}_5\text{H}$  at  $\delta$  7.16 ppm. In the paramagnetic complexes, all peaks are singlets. In parentheses are listed  $T_2$  values in ms (calculated as  $(\pi\Delta\nu_{1/2})^{-1}$ ),<sup>17,37</sup> integrations, and assignments. In some cases, overlapping peaks prevented  $T_2$  determinations. Coupling constants in the spectra of the diamagnetic complexes are reported in Hertz. IR spectra were recorded on a Mattson Instruments 6020 Galaxy Series FTIR using solution cells with CsF windows. UV–vis spectra were measured on a Cary 50 spectrophotometer, using screw-cap cuvettes. Solution magnetic susceptibilities were determined by the Evans method.<sup>41</sup> Elemental analyses were determined by Desert Analytics, Tucson, AZ.

Pentane, diethyl ether, tetrahydrofuran (THF), and toluene were purified by passage through activated alumina and “deoxygenizer” columns from Glass Contour Co. (Laguna Beach, CA). Deuterated benzene was first dried over  $\text{CaH}_2$  and then over Na/benzophenone and then vacuum-transferred into a storage container. Before use, an aliquot of each solvent was tested with a drop of sodium benzophenone ketyl in THF solution. Celite was dried overnight at  $200^\circ\text{C}$  under vacuum.  $\text{LiCH}_2\text{CMe}_3$  was prepared from neopentyl chloride and lithium in pentane and purified by sublimation. Grignard reagents (1–2 M in  $\text{Et}_2\text{O}$  or THF) were obtained from Aldrich and used without further purification.

**Improved Synthesis of  $\text{LFeCl}$ .** A 200 mL Schlenk flask was charged with  $\text{FeCl}_2(\text{THF})_{1.5}$ <sup>42</sup> (8.0 g, 34 mmol),  $\text{LiL}(\text{THF})$ <sup>43</sup> (20 g, 34 mmol), and toluene (150 mL). The reaction mixture became red. The reaction mixture was then heated at  $100^\circ\text{C}$  for 24 h to form a dark red solution. The solvent was removed in vacuo, and the red solid residue was transferred to a glass thimble, which was placed in a Soxhlet extractor. Continuous extraction of the residue with hot diethyl ether until the extracting solvent was clear (1–2 days) led to the formation

(40) Fekl, U.; Kaminsky, W.; Goldberg, K. I. *J. Am. Chem. Soc.* **2001**, 123, 6423–6424.

(41) Baker, M. V.; Field, L. D.; Hambley, T. W. *Inorg. Chem.* **1988**, 27, 7.

(42) Kern, R. J. *J. Inorg. Nucl. Chem.* **1962**, 24, 1105.

(43) Budzelaar, P. H. M.; van Oort, A. B.; Orpen, A. G. *Eur. J. Inorg. Chem.* **1998**, 1485.



of a red slurry and left a gray solid behind. The solvent was then reduced to ca. 50 mL, and the red solid was isolated by filtration (17.0 g). Further product was obtained by crystallization from the mother liquor at  $-35^{\circ}\text{C}$ . The total yield is 19.0 g (94%).  $^1\text{H}$  NMR ( $\text{C}_6\text{D}_6$ ):  $\delta$  109 (0.32, 1H, CH); 43 (0.64, 9H,  $\text{C}(\text{CH}_3)_3$ ), 0 (0.13, 4H, *m*-H),  $-29$  (2.1, 12H,  $\text{CH}(\text{CH}_3)_2$ ),  $-111$  (1.3, 2H, *p*-H),  $-115$  (0.27, 12H,  $\text{CH}(\text{CH}_3)_2$ ),  $-116$  (4H,  $\text{CH}(\text{CH}_3)_2$ ).

**General Synthesis of  $\text{LFeR}$  ( $\text{R} = \text{Et}$ ,  $^i\text{Pr}$ ).** To a red slurry of  $\text{LFeCl}$  in diethyl ether (10 mL) was added via syringe 1 molar equiv of the appropriate Grignard reagent solution in THF. The red color of the reaction mixture faded to orange, with the formation of a white precipitate. The reaction mixture was stirred overnight and the solvent removed in vacuo. The residue was extracted with pentane and filtered through a plug of Celite to give an orange solution. The solution was then concentrated (ca. 2 mL) and warmed to dissolve the product. Orange crystals were isolated after cooling to  $-35^{\circ}\text{C}$ .

**$\text{LFeEt}$ .** Yield: 80%.  $^1\text{H}$  NMR ( $\text{C}_6\text{D}_6$ ):  $\delta$  129 (0.28, 1H, CH), 42 (0.80, 18H,  $\text{C}(\text{CH}_3)_3$ ),  $-5$  (1.6, 4H, *m*-H),  $-29$  (0.13, 12H,  $\text{CH}(\text{CH}_3)_2$ ),  $-112$  (1.1, 2H, *p*-H),  $-116$  (0.24, 4H,  $\text{CH}(\text{CH}_3)_2$ ),  $-136$  (0.32, 12H,  $\text{CH}(\text{CH}_3)_2$ ).  $\mu_{\text{eff}}$  (Evans,  $\text{C}_6\text{D}_6$ ): 4.9(3)  $\mu_{\text{B}}$ . UV-vis (pentane): 517 nm ( $\epsilon = 0.59(2) \text{ mM}^{-1} \text{ cm}^{-1}$ ). Anal. Calcd for  $\text{C}_{37}\text{H}_{58}\text{N}_2\text{Fe}$  (586.71): C, 75.74; H, 9.96; N, 4.77. Found: C, 74.34; H, 9.68; N, 4.68. Despite repeated attempts, we were not able to obtain an accurate microanalysis on spectroscopically pure material.

**$\text{LFe}^i\text{Pr}$ .** Yield: 92%.  $^1\text{H}$  NMR ( $\text{C}_6\text{D}_6$ ):  $\delta$  128 (0.29, 1H, CH), 45 (0.80, 18H,  $\text{C}(\text{CH}_3)_3$ ),  $-7$  (1.1, 4H, *m*-H),  $-27$  (1.6, 12H,  $\text{CH}(\text{CH}_3)_2$ ),  $-104$  (1.6, 2H, *p*-H),  $-110$  (4H,  $\text{CH}(\text{CH}_3)_2$ ),  $-139$  (0.29, 12H,  $\text{CH}(\text{CH}_3)_2$ ).  $\mu_{\text{eff}}$  (Evans,  $\text{C}_6\text{D}_6$ ): 5.4(3)  $\mu_{\text{B}}$ . UV-vis (pentane): 515 nm ( $\epsilon = 0.53(2) \text{ mM}^{-1} \text{ cm}^{-1}$ ). Anal. Calcd for  $\text{C}_{38}\text{H}_{60}\text{N}_2\text{Fe}$  (600.74): C, 75.97; H, 10.07; N, 4.66. Found: C, 75.81; H, 9.49; N, 4.63.

**$\text{LFeCH}_2^i\text{Bu}$ .** A clear solution of  $\text{LiCH}_2^i\text{Bu}$  (37 mg, 472  $\mu\text{mol}$ ) in  $\text{Et}_2\text{O}$  (5 mL) was added to a red slurry of  $\text{LFeCl}$  (280 mg, 472  $\mu\text{mol}$ ) in  $\text{Et}_2\text{O}$  (10 mL). The reaction mixture immediately became orange with the formation of a white precipitate. After it was stirred for 2 h at room temperature, the mixture was filtered through a plug of Celite to give an orange solution. The solvent was removed under vacuum, and the residue was dissolved in hot pentane (4 mL). The product was then crystallized in two crops at  $-35^{\circ}\text{C}$  to give an orange solid (240 mg, 81%).  $^1\text{H}$  NMR ( $\text{C}_6\text{D}_6$ ):  $\delta$  129 (0.29, 9H,  $\text{CH}_2\text{C}(\text{CH}_3)_3$ ), 45 (0.91, 18H,  $\text{C}(\text{CH}_3)_3$ ),  $-7$  (1.1, 4H, *m*-H),  $-27$  (2.1, 12H,  $\text{CH}(\text{CH}_3)_2$ ),  $-104$  (1.3, 2H, *p*-H),  $-110$  (0.19, 4H,  $\text{CH}(\text{CH}_3)_2$ ),  $-139$  (0.32, 12H,  $\text{CH}(\text{CH}_3)_2$ ).  $\mu_{\text{eff}}$  (Evans,  $\text{C}_6\text{D}_6$ ): 5.5(3)  $\mu_{\text{B}}$ . UV-vis (pentane): 520 nm ( $\epsilon = 0.58(2) \text{ mM}^{-1} \text{ cm}^{-1}$ ). Anal. Calcd for  $\text{C}_{40}\text{H}_{64}\text{N}_2\text{Fe}$  (628.79): C, 76.40; H, 10.26; N, 4.46. Found: C, 76.86; H, 10.33; N, 4.44.

**$\text{LFe}(\text{CO})_2(\text{COMe})$ .** A resealable flask was charged with  $\text{LFeMe}$  (200 mg, 349  $\mu\text{mol}$ ) and diethyl ether (15 mL) to give an orange solution, which was frozen at  $-196^{\circ}\text{C}$ . The headspace was evacuated and refilled with CO to approximately 1 atm. The solvent was then thawed to give a red solution that was stirred at room temperature for 4 h. The volatiles were removed in vacuo and the red residue dissolved in a diethyl ether/pentane mixture. Red crystals (205 mg, 90%) were grown at  $-35^{\circ}\text{C}$ .  $^1\text{H}$  NMR ( $\text{C}_6\text{D}_6$ ): major isomer,  $\delta$  7.08–7.16 (m, 6H, Ar *H*), 6.67 (s, 1H, backbone *CH*), 3.47 (dt,  $J_{\text{HH}} = 6$ ,  $J_{\text{HH}} = 6$ , 2H,  $\text{CH}(\text{CH}_3)_2$ ), 2.65 (s, 3H,  $\text{COCH}_3$ ), 2.59 (dt,  $J_{\text{HH}} = 6$ ,  $J_{\text{HH}} = 6$ , 2H,  $\text{CH}(\text{CH}_3)_2$ ), 1.46 (d,  $J_{\text{HH}} = 6$ , 6H,  $\text{CH}(\text{CH}_3)_2$ ), 1.45 (d,  $J_{\text{HH}} = 6$ , 6H,  $\text{CH}(\text{CH}_3)_2$ ), 1.34 (d,  $J_{\text{HH}} = 6$ , 6H,  $\text{CH}(\text{CH}_3)_2$ ), 1.30 (s, 18H,  $\text{C}(\text{CH}_3)_3$ ), 1.23 (d,  $J_{\text{HH}} = 6$ , 6H,  $\text{CH}(\text{CH}_3)_2$ ); minor isomer,  $\delta$  7.08–7.16 (m, 6H, Ar *H*), 6.39 (s, 1H, backbone *CH*), 3.64 (dt,  $J_{\text{HH}} = 6$ ,  $J_{\text{HH}} = 6$ , 2H,  $\text{CH}(\text{CH}_3)_2$ ), 3.47 (s, 3H,  $\text{COCH}_3$ ), 2.51 (dt,  $J_{\text{HH}} = 6$ ,  $J_{\text{HH}} = 6$ , 2H,  $\text{CH}(\text{CH}_3)_2$ ), 1.55 (d,  $J_{\text{HH}} = 6$ , 6H,  $\text{CH}(\text{CH}_3)_2$ ), 1.48 (d,  $J_{\text{HH}} = 6$ , 6H,  $\text{CH}(\text{CH}_3)_2$ ), 1.33 (d,  $J_{\text{HH}} = 6$ , 6H,  $\text{CH}(\text{CH}_3)_2$ ), 1.25 (s, 18H,  $\text{C}(\text{CH}_3)_3$ ), 1.23 (d,  $J_{\text{HH}} = 6$ , 6H,  $\text{CH}(\text{CH}_3)_2$ ). IR (pentane): 1998, 1934 (major isomer), 2012, 1948 (minor), 1687  $\text{cm}^{-1}$ . Anal.

Calcd for  $\text{C}_{39}\text{H}_{56}\text{N}_2\text{O}_3\text{Fe}$ : C, 71.33; H, 8.59; N, 4.27. Found: C, 71.57; H, 8.23; N, 4.13.

**Reaction of  $\text{LFeR}$  ( $\text{R} = \text{Me}$ ,  $^n\text{Pn}$ ,  $^i\text{Pr}$ ) with  $^{13}\text{CO}$ .** In a resealable NMR tube,  $\text{LFeR}$  ( $\text{R} = \text{Me}$ ,  $^n\text{Pn}$ ,  $^i\text{Pr}$ ) (5–10 mg) was dissolved in  $\text{C}_6\text{D}_6$  (0.5 mL) to give an orange solution. The solution was frozen and the headspace evacuated and back-filled with  $^{13}\text{CO}$  (ca. 1 atm). The solution was thawed and mixed, resulting in a color change to red. The complexes were characterized by  $^1\text{H}$  and  $^{13}\text{C}$  NMR and IR spectroscopy.

**$\text{LFe}^{(13}\text{CO})_2(^{13}\text{COMe})$ .** Major isomer:  $^{13}\text{C}\{^1\text{H}\}$  NMR ( $\text{C}_6\text{D}_6$ )  $\delta$  248.1 (t,  $J_{\text{CC}} = 9.0$ ,  $\text{COMe}$ ), 208.0 (d,  $J_{\text{CC}} = 9.0$ , CO);  $^{13}\text{C}$  NMR ( $\text{C}_6\text{D}_6$ )  $\delta$  248.1 (tq,  $J_{\text{CC}} = 9.0$ ,  $J_{\text{CH}} = 5.1$ ,  $\text{COMe}$ ), 208.0 (d,  $J_{\text{CC}} = 9.0$ , CO); IR (pentane) 1949, 1884, 1665  $\text{cm}^{-1}$ . Minor isomer:  $^{13}\text{C}\{^1\text{H}\}$  NMR ( $\text{C}_6\text{D}_6$ )  $\delta$  251.8 (tq,  $J_{\text{CC}} = 9.4$ ,  $J_{\text{CH}} = 4.5$ ,  $\text{COMe}$ ), 206.0 (d,  $J_{\text{CC}} = 9.4$ , CO); IR (pentane) 1968, 1908, 1665  $\text{cm}^{-1}$ .

**$\text{LFe}^{(13}\text{CO})_2(^{13}\text{COCH}_2^i\text{Bu})$ .** Major isomer:  $^1\text{H}$  NMR ( $\text{C}_6\text{D}_6$ )  $\delta$  7.00–7.13 (m, 6H, Ar *H*), 6.79 (s, 1H, backbone *CH*), 3.35 (dt,  $J_{\text{HH}} = 6$ ,  $J_{\text{HH}} = 6$ , 2H,  $\text{CH}(\text{CH}_3)_2$ ), 3.24 (s, 2H,  $\text{CH}_2$ ), 2.31 (dt,  $J_{\text{HH}} = 6$ ,  $J_{\text{HH}} = 6$ , 2H,  $\text{CH}(\text{CH}_3)_2$ ), 1.40 (d, 6H,  $\text{CH}(\text{CH}_3)_2$ ), 1.40 (d,  $J_{\text{HH}} = 6$ , 6H,  $\text{CH}(\text{CH}_3)_2$ ), 1.30 (d,  $J_{\text{HH}} = 6$ , 6H,  $\text{CH}(\text{CH}_3)_2$ ), 1.29 (s, 18H,  $\text{C}(\text{CH}_3)_3$ ), 1.25 (d,  $J_{\text{HH}} = 6$ , 6H,  $\text{CH}(\text{CH}_3)_2$ ), 1.10 (d, 9H,  $\text{CH}_2\text{C}(\text{CH}_3)_3$ );  $^{13}\text{C}\{^1\text{H}\}$  NMR ( $\text{C}_6\text{D}_6$ )  $\delta$  247.6 (t,  $J_{\text{CC}} = 8.5$ ,  $\text{COCH}_2^i\text{Bu}$ ), 209.3 (d,  $J_{\text{CC}} = 8.5$ , CO); IR (pentane) 1973, 1915, 1654  $\text{cm}^{-1}$ . Minor isomer:  $^1\text{H}$  NMR ( $\text{C}_6\text{D}_6$ , not all peaks could be observed)  $\delta$  7.00–7.13 (m, 6H, Ar *H*), 5.62 (s, 1H, backbone *CH*), 3.72 (dt,  $J_{\text{HH}} = 6$ ,  $J_{\text{HH}} = 6$ , 2H,  $\text{CH}(\text{CH}_3)_2$ ), 3.60 (dt,  $J_{\text{HH}} = 6$ ,  $J_{\text{HH}} = 6$ , 2H,  $\text{CH}(\text{CH}_3)_2$ ), 1.63 (d, 6H,  $\text{CH}(\text{CH}_3)_2$ ), 1.55 (d,  $J_{\text{HH}} = 6$ , 6H,  $\text{CH}(\text{CH}_3)_2$ ), 1.22 (s, 3H,  $\text{CH}_2\text{C}(\text{CH}_3)_3$ );  $^{13}\text{C}\{^1\text{H}\}$  NMR ( $\text{C}_6\text{D}_6$ )  $\delta$  249.3 (t,  $J_{\text{CC}} = 8.3$ ,  $\text{COCH}_2^i\text{Bu}$ ), 206.4 (d,  $J_{\text{CC}} = 8.3$ , 2C, CO).

**$\text{LFe}^{(13}\text{CO})_2(^{13}\text{CO}^i\text{Pr})$ .**  $^1\text{H}$  NMR ( $\text{C}_6\text{D}_6$ ):  $\delta$  7.01–7.14 (m, 6H, Ar *H*), 6.75 (s, 1H, backbone *CH*), 3.43 (m,  $J_{\text{HH}} = 6$ , 2H,  $\text{CH}(\text{CH}_3)_2$ ), 3.29 (dt,  $J_{\text{HH}} = 6$ , 1H,  $\text{CH}(\text{CH}_3)_2$ ), 2.36 (dt,  $J_{\text{HH}} = 6$ , 2H,  $\text{CH}(\text{CH}_3)_2$ ), 1.37 (d,  $J_{\text{HH}} = 6$ , 3H,  $\text{CH}(\text{CH}_3)_2$ ), 1.35 (d,  $J_{\text{HH}} = 6$ , 3H,  $\text{CH}(\text{CH}_3)_2$ ), 1.33 (d,  $J_{\text{HH}} = 6$ , 3H,  $\text{CH}(\text{CH}_3)_2$ ), 1.27 (d,  $J_{\text{HH}} = 6$ , 3H,  $\text{CH}(\text{CH}_3)_2$ ), 1.18 (s, 18H,  $\text{C}(\text{CH}_3)_3$ ), 1.16 (d,  $J_{\text{HH}} = 6$ , 3H,  $\text{CH}(\text{CH}_3)_2$ ), 1.11 (d, 6H,  $\text{CH}(\text{CH}_3)_2$ );  $^{13}\text{C}\{^1\text{H}\}$  NMR ( $\text{C}_6\text{D}_6$ ):  $\delta$  252.8 (t,  $J_{\text{CC}} = 8.5$ ,  $\text{CO}^i\text{Pr}$ ), 210.0 (d,  $J_{\text{CC}} = 8.5$ , CO). IR (pentane): 1950, 1886, 1619  $\text{cm}^{-1}$ .

**X-ray Structural Determination of  $\text{LFeCH}_2^i\text{Bu}$ ,  $\text{LFe}^i\text{Pr}$ , and  $\text{LFe}(\text{CO})_2(\text{COMe})$ .** Crystalline samples of the three complexes were grown from pentane solutions at  $-35^{\circ}\text{C}$ . All samples were rapidly mounted under Paratone-8277 onto glass fibers and immediately placed in a cold nitrogen stream at  $-80^{\circ}\text{C}$  on the X-ray diffractometer. The X-ray intensity data were collected on a standard Bruker SMART CCD area detector system equipped with a normal-focus Mo-target X-ray tube operated at 2.0 kW (50 kV, 40 mA). A total of 1321 frames of data (1.3 hemispheres) were collected using a narrow-frame method with scan widths of  $0.3^{\circ}$  in  $\omega$  and exposure times of 30 s/frame for  $\text{LFe}^i\text{Pr}$  and  $\text{LFe}(\text{CO})_2(\text{COMe})$ , and 60 s/frame for  $\text{LFeCH}_2^i\text{Bu}$ , with a detector-to-crystal distance of 5.09 cm. Frames were integrated to a maximum  $2\theta$  angle of  $56.5^{\circ}$  with the Bruker SAINT program. Laue symmetry revealed monoclinic crystal systems for  $\text{LFeCH}_2^i\text{Bu}$  and  $\text{LFe}^i\text{Pr}$  and a triclinic system for  $\text{LFe}(\text{CO})_2(\text{COMe})$ . The final unit cell parameters were determined from the least-squares refinement of three-dimensional centroids of  $>3400$  reflections for each crystal.<sup>44</sup> Data were corrected for absorption with SADABS.<sup>45</sup>

The space groups were assigned as  $P2_1/n$  (No. 14) for  $\text{LFeCH}_2^i\text{Bu}$  and  $\text{LFe}^i\text{Pr}$ , and  $P\bar{1}$  (No. 2) for  $\text{LFe}(\text{CO})_2(\text{COMe})$ , and the structures were solved by direct methods using SIR92<sup>46</sup> and refined employing full-matrix least squares on  $F^2$  (SHELXTL-NT,<sup>47</sup> version 5.10). The disordered methyl

(44) It has been noted that the integration program SAINT produces cell constant errors that are unreasonably small, since systematic error is not included. More reasonable errors might be estimated at 10× the reported value.

(45) The SADABS program is based on the method of Blessing; see: Blessing, R. H. *Acta Crystallogr., Sect. A* **1995**, *51*, 33.

carbon atoms C(82) and C(82A) in  $\text{LFe}(\text{CO})_2(\text{COMe})$  were refined anisotropically using the PART instruction. All other non-H atoms in all three complexes were refined with anisotropic thermal parameters. Hydrogen atoms were included in idealized positions. The structures were refined to goodness of fit (GOF) values and final residuals found in Table 1.

---

(46) Altomare, A.; Cascarano, G.; Giacovazzo, C.; Gualardi, A. *J. Appl. Crystallogr.* **1993**, *26*, 343–350.

(47) SHELXTL NT: Structure Analysis Program, version 5.10; BRUKER-AXS, Madison, WI, 1995.

**Acknowledgment.** We thank the National Science Foundation (Grant No. CHE-0134658) and the University of Rochester for financial support.

**Supporting Information Available:** Tables giving X-ray crystallographic information; these data are also available in CIF format. This material is available free of charge via the Internet at <http://pubs.acs.org>.

OM020571V